Lithium isotopic systematics of granites and pegmatites from the Black Hills, South Dakota

Fang-Zhen Teng[1], William F. McDonough[1], Roberta L. Rudnick[1], Richard J. Walker[1] and Mona-Liza C. Sirbescu[2]

1. Geochemistry Laboratory, Department of Geology, University of Maryland, College Park, MD 20742, U.S.A.

2. Department of Geology, Central Michigan University, Mt. Pleasant, MI 48859, U.S.A.

Text word count: 5725

Figures: eight

Tables: four

Submitted to American Mineralogist (4/8/06)

(Revised version)

Email: tfz@geol.umd.edu

Tel: +1-301-405-2707

Fax: +1-301-405-3597

Abstract

In order to study Li isotopic fractionation during granite differentiation and late-stage pegmatite evolution, Li isotopic compositions and concentrations have been measured for the S-type Harney Peak Granite, the spatially associated Tin Mountain pegmatite and possible metasedimentary source rocks in the Black Hills, South Dakota, USA. The Harney Peak Granite is isotopically heterogeneous, with δ^7Li varying from -3.1 to +6.6. The δ^7Li values of Proterozoic metasedimentary rocks that are possible sources of the Harney Peak Granite range from -3.1 to +2.5 and overlap with post-Archean shales and the Harney Peak Granite. For the granite suite, there is no correlation between δ^7Li and elements indicative of degrees of granite differentiation (SiO_2, Li, Rb, etc.). The Li isotopic composition of the Harney Peak Granite, therefore, appears to reflect the source composition.

Minerals from the zoned Tin Mountain pegmatite have extremely high Li contents and heavier Li isotopic compositions than the granite or surrounding Black Hills metasedimentary rocks. The heavier compositions may reflect Li isotopic fractionation resulting from extensive crystal-melt fractionation. Lithium concentrations decrease in the order: spodumene (~3.7 wt %), muscovite (0.2 to 2.0 wt.%), plagioclase (100-1100 ppm), quartz (30-140 ppm). Plagioclase, muscovite, and spodumene in all zones display a relatively narrow range in δ^7Li of +7.9 to +11.4. In contrast, quartz is isotopically heavier and more variable (+14.7 to +21.3), with δ^7Li showing an inverse correlation with Li concentration. This correlation reflects the mixing of isotopically heavy Li in quartz and lighter Li in fluid inclusions, as documented by fluid inclusion data (δ^7Li = +8.1 to +13.4 and Li of 280 to 3960 ppm). Extrapolation of this trend to an estimated intrinsic Li

concentration in quartz of <30 ppm, yields an inferred δ^7Li for fluid inclusion-free quartz of >+21. The large difference in δ^7Li between quartz and other minerals may reflect ^{7}Li preference for less highly coordinated sites, which have higher bond-energies (i.e., the two- or four-fold site in quartz vs. higher coordination number sites in other minerals). Comparison of the Li isotopic composition of fluid inclusions with that of the wall zone Tin Mountain pegmatite suggests ~4‰ isotopic fractionation during fluid exsolution, which agrees with the results derived from studies of hydrothermal alteration of basalts.

1. Introduction

Recent studies have significantly increased our knowledge of Li isotope geochemistry by documenting the Li isotopic variations in different geological reservoirs, and illuminating the processes that may produce these variations (see recent reviews by Chan, 2004; Elliott et al., 2004; Tomascak, 2004). These studies have shown that Li isotopes in the outer layers of the Earth (hydrosphere, crust and lithospheric mantle) can be strongly fractionated, with observed Li isotope fractionation in the near–surface environment of > 60‰ (Tomascak, 2004).

Lithium isotopic fractionation has been documented in a variety of geological processes, such as weathering (Huh et al., 2004; Kisakurek et al., 2004; Pistiner and Henderson, 2003; Rudnick et al., 2004), hydrothermal alteration (Bouman et al., 2004; Chan and Kastner, 2000; Chan et al., 1992; 1993; 1994; 2002; Foustoukos et al., 2004; James et al., 2003; Seyfried Jr. et al., 1998; Williams and Hervig, 2005), metamorphic dehydration (Benton et al., 2004; Teng et al., 2004b; 2006b; Zack et al., 2003) and diffusion (Lundstrom et al., 2005; Richter et al., 2003; Teng et al., 2006a). In contrast,

little isotopic fractionation is inferred to occur during high temperature igneous differentiation, be it in basaltic (Tomascak et al., 1999) or granitic (Bryant et al., 2004; Teng et al., 2004a; Tomascak et al., 1995) systems. However, large Li isotopic fractionations (up to 20‰) between minerals and hydrothermal fluids may occur in aqueous fluid-rich granitic pegmatite systems at relatively low temperatures (Lynton et al., 2005).

In order to further examine Li isotope fractionation in evolved granitic systems, including relatively wet, low temperature pegmatites, we studied well-characterized samples of the highly differentiated Harney Peak Granite, the spatially associated, Li-rich Tin Mountain pegmatite, and metasedimentary country rocks from the Black Hills, South Dakota. The goals of this study are to study Li isotopic fractionation during granite differentiation and late-stage pegmatite evolution and use Li isotopes to provide additional insight into the origin and evolution of Harney Peak Granite and Tin Mountain pegmatite.

2. Geological background and samples

The Black Hills Precambrian terrane consists of two Late Archean meta-granites (Little Elk and Bear Mountain), early Proterozoic metasedimentary and metavolcanic rocks, and the Proterozoic (ca. 1700 Ma) Harney Peak Granite, which is surrounded by thousands of simple and zoned pegmatites (Duke et al., 1990; Norton and Redden, 1990; Redden et al., 1985; Shearer et al., 1987a; Walker et al., 1986b). We discuss each of these units in turn.

2.1 Country rocks

The dominant rock types in this region are early Proterozoic micaceous and quartzose schists, derived from shales and graywackes, with the highest metamorphic grade reaching second-sillimanite zone. The schist is composed of quartz, biotite, plagioclase and occasional minor muscovite, and has considerable variation in modal mineralogy. In order to characterize the compositional variations within the metamorphic terrane, four quartz mica schists sampled from throughout the southern Black Hills were measured for both Li concentration and isotopic composition (Fig.1). Samples 23-2 and 40-1A were collected near the first sillimanite isograd. Samples WC-4 and 26-2 were collected near the second sillimanite isograd. These samples were taken from regions well away from most granitic outcrops and have not been affected by interactions with pegmatites, granites or fluids derived therefrom (Teng et al., 2006a), and are therefore representative of their original compositions.

Two late Archean granites, the Little Elk granite and the Bear Mountain granite, crop out in the region. The little Elk granite, with a U-Pb zircon age of ~2560 Ma (Zartman and Stern, 1967), is medium-grained, gneissic, and comprised primarily of plagioclase, microcline, quartz, biotite and muscovite (Walker et al., 1986a). The Bear Mountain granite, with a Rb-Sr whole-rock age of ~2450 Ma (Ratte and Zartman, 1975), is medium-grained to pegmatitic, consisting predominantly of plagioclase, quartz, microcline, muscovite, biotite and trace apatite (Walker et al., 1986a). These two Archean plutons have experienced at least two episodes of metamorphism caused by the intrusion of the Proterozoic Harney Peak Granite and Tertiary rhyolite and quartz monzonite in the northern Black Hills (Zartman et al., 1964). Samples from both plutons

have been measured to characterize the δ^7Li of the late Archean crust (Fig. 1). No other Archean rock types are known to crop out in this region.

2.2 Harney Peak Granite

The Proterozoic Harney Peak Granite is the dominant exposed granitic rock. It does not form a single plutonic body but instead consists of hundreds of individual dikes and sills. The Harney Peak Granite is both texturally and compositionally diverse. It has a peraluminous composition, with low Ca and high water content, and $\delta^{18}O > 10$, consistent with derivation from partial melting of metasedimentary rocks (Nabelek and Bartlett, 1998; Walker et al., 1986a). Nabelek et al (1992b) divide the Harney Peak Granite into two groups with different sources: biotite granite in the core of the complex, with low $\delta^{18}O$ (+11.5 ±0.6), and tourmaline granite on the periphery of the complex, with high $\delta^{18}O$ (+13.2 ±0.8). Lead isotopes indicate that the biotite granite was derived from melting of late Archean crust, while the tourmaline granite was derived from melting of Proterozoic crust (Krogstad et al., 1993). Two potential sources for the Harney Peak Granite are sediments derived from Archean granites, and the surrounding Proterozoic country rocks (Nabelek and Bartlett, 1998; Walker et al., 1989).

Twenty-five samples, covering the compositional spectrum of the Harney Peak Granite, were measured in order to obtain a clear picture of δ^7Li variations in this heterogeneous granite. In addition, four samples of simple pegmatites from the surrounding region were also measured (Fig. 1). One of these, a pegmatitic vein (WC-9), was likely produced *in situ* from partial melting of the enclosing metasedimentary rock (WC-4), probably due to heating resulting from the intrusion of the Harney Peak Granite

(Shearer et al., 1987b). This sample pair thus allows evaluation of the amount of Li isotopic fractionation accompanying partial melting. All samples are fresh, with H and O isotope data showing no evidence for interaction with meteoric water (Nabelek et al., 1992b).

2.3 Tin Mountain pegmatite

The Li-rich Tin Mountain pegmatite is a zoned pegmatite that discordantly intrudes both metasedimentary rocks and amphibolites, and crops out ~12 km to the southwest of the main body of the Harney Peak Granite. Walker et al (1986b) show that this pegmatite consists of five major zones, with the wall zone forming a shell that encloses four inner zones (Fig. 2). Quartz, plagioclase and Li-rich muscovite occur in all five zones; potassium feldspar dominates the 1st and 2nd intermediate zones while spodumene mainly occurs in the 3rd intermediate zone and core. Crystallization of the wall zone occurred first, as indicated by its relatively low incompatible element concentrations (Rb, Cs, and Li) and high compatible element concentrations (Ba and Sr), followed by the first intermediate zone. The remaining intermediate zones and the core then crystallized simultaneously. The fracture fillings crystallized last (Walker et al., 1986b). The estimated crystallization temperature varies from >600 ^{o}C in the wall zone to 500 ^{o}C in the core, based on oxygen isotopic thermometry (Walker et al., 1986b). More recent temperature estimates based on fluid and melt inclusions yield even lower crystallization temperatures, down to 340 ^{o}C (Sirbescu and Nabelek, 2003a; 2003b).

Walker et al. (1989) utilize trace element and isotope (O, Nd, Sr) data to suggest two possible origins for the parental melts of this pegmatite: (1) Low degree partial melts

of metasedimentary rocks that experienced moderate extents of fractional or equilibrium crystallization or (2) derivation from the Harney Peak Granite via a complex, multi-stage crystal-liquid fractional crystallization process, such as progressive equilibrium crystallization. The different zones of the Tin Mountain pegmatite resulted from extensive crystal-melt-fluid fractionation (Walker et al., 1986b).

Eight samples including quartz, plagioclase and muscovite from different zones of the Tin Mountain pegmatite have been studied previously by Tomascak et al. (1995) using a method with relatively low precision (± 2.1‰, 2σ). Here, more samples from this pegmatite (n = 33) are measured using a method with higher precision (≤ ± 1‰, 2σ). Quartz, plagioclase, muscovite and spodumene from all major zones and fracture fillings of the Tin Mountain Pegmatite and eight fluid inclusion samples in quartz from the 1st, 2nd, 3rd intermediate and core zones were measured for δ^7Li and Li concentration. In addition, in order to characterize the Li isotopic composition of the bulk pegmatite, three whole rock composites from the wall zone were also measured. Two (9-2 and 10-3) were powdered from 5 kg of rock and one (43-1) was produced from 100 kg of rock.

3. Analytical methods

All sample powders are the same as those used in previous studies (Krogstad and Walker, 1996; Nabelek et al., 1992a; 1992b; Walker et al., 1986a; 1986b; 1989) except three of the pegmatite minerals, which were drilled directly from rock slabs, since previous powders were exhausted (see Table 2 for details). Fluid inclusions were extracted by the crush and leach method at Central Michigan University, using a method modified from Bottrell et al.(1988). The leachates were extracted by manually crushing 2

g of handpicked and cleaned quartz grains in 4 ml of distilled-deionized water with a resistance of >18.1 MΩ·cm, centrifuged and then filtered using nylon filters with 0.45 μm pores. Based on traditional textural analysis of fluid inclusion populations and homogenization temperatures, primary inclusions of magmatic origin dominate the quartz samples selected for the crush-leach analysis (>90%).

Lithium isotopic analyses were performed at the Geochemistry Laboratory of the University of Maryland, College Park. The fluid inclusion leachates were dried and re-dissolved in 4M HCl, in preparation for chromatographic separation. Sample powders were dissolved in a ~ 3:1 mixture of concentrated HF-HNO_3 in Savillex screw-top beakers overnight on a hot plate (T< 120 ^{o}C), followed by replenishment of the dried residua with concentrated HNO_3 overnight and dried again, then picked up in concentrated HCl until solutions were clear. The solutions were then dried down and re-dissolved in 4 M HCl, in preparation for chromatographic separation. Around 100 ng Li in 1 ml 4 M HCl was loaded on the first column. Lithium was eluted though three sets of columns, each containing 1 ml of cation exchange resin (BioRad AG50W-x12) following the first three column procedures described by Moriguti and Nakamura (1998). Columns were calibrated using samples with different matrixes (e.g., peridotite, basalt, granite and pure Li solution). In order to check Li yields, before/after cuts for each sample were collected and analyzed by single collector ICP-MS (Thermo Finnigan Element 2). With ~100 ng of sample Li loaded (corresponding to 1 to10 mg of sample), the column procedure separates Li from other elements with >98% yield.

The MC-ICP-MS analysis protocol is similar to that reported in Teng et al. (2004a). In brief, prior to Li isotopic analyses, the Na/Li voltage ratio of each solution is

evaluated semi-quantitatively with the mass spectrometer. Solutions with a Na/Li voltage ratio ≥ 5 are reprocessed through the 3rd column. Purified Li solutions (~100 ppb Li in 2% HNO_3 solutions) are introduced to the Ar plasma using an auto-sampler (ASX-100® Cetac Technologies) through a desolvating nebulizer (Aridus® Cetac Technologies) fitted with a PFA spray chamber and micro-nebulizer (Elemental Scientific Inc.). Samples were analyzed using a Nu-Plasma MC-ICP-MS (Belshaw et al., 1998), with ^{7}Li and ^{6}Li measured simultaneously in separate Faraday cups. Each sample analysis is bracketed by measurements of the L-SVEC (a Li carbonate standard, Flesch et al., 1973) having a similar solution concentration and acid strength (although tests revealed that standard/sample concentration ratios can vary by up to an order of magnitude without detriment to the measurement). Two other Li standards (e.g., the in-house Li-UMD1, a purified Li solution from Alfa Aesar®, and IRMM-016 (Qi et al., 1997)) are routinely analyzed during the course of each analytical session. A rock standard (AO-12, a Post Archean Australian shale (PAAS), Teng et al., 2004a), is also routinely analyzed for quality control purposes. International rock standard BCR-1 was also measured during the course of this study. The in-run precision on $^{7}Li/^{6}Li$ measurements is ≤ ± 0.2‰ for two blocks of 20 ratios each, with no apparent instrumental fractionation. The external precision, based on 2 σ of repeat runs of both pure Li standard solutions and natural rocks, is < ± 1.0‰. For example, pure Li standard solutions (IRMM-016 and UMD-1) always have values falling within previous established ranges (-0.1 ± 0.2‰ and +54.7 ± 1‰, Teng et al., 2004a); AO-12 gives $\delta^{7}Li$ = +3.5 ± 0.6 (2 σ, n = 36 runs with 4 replicate sample preparations); and BCR-1 gives $\delta^{7}Li$ = +2.0 ± 0.7 (2 σ, n = 10 runs) where $\delta^{7}Li$ is defined as $\delta^{7}Li = [(^{7}Li/^{6}Li)_{Sample} / (^{7}Li/^{6}Li)_{LSVEC} - 1] \times 1000$.

Lithium concentrations in mineral separates and whole rocks were determined by voltage comparison with that measured for 100 ppb or 50 ppb L-SVEC standards and then adjusting for sample weight. The precision is better than ± 10% except for spodumene (Teng et al., 2004a). Lithium concentration in spodumene is very high, which makes it difficult to precisely constrain the sample weight loaded onto the column hence concentration. For this reason, the Li concentration in spodumene reported here is calculated from its standard molecular formula. The bulk Li concentrations in leachates were analyzed using a Dionex DX320 ion chromatograph, equipped with a CSRS®-ULTRA 4 mm suppressor combined with CG12A-CS12A (4 mm) chromatographic columns, with an uncertainty of < 5%. Chlorine concentrations were also analyzed by chromatography on separate sample aliquots, using an ASRS®-ULTRA 4 mm suppressor combined with AG9-HC – AS9-HC (4mm) columns, with an uncertainty of < 3%. Lithium concentrations in fluid inclusions were calculated by using Li and Cl concentrations in leachates and the average salinity of Tin Mountain inclusions (4.5 wt% $NaCl_{eq}$) measured by microthermometry (Sirbescu and Nabelek, 2003a).

4. Results

The Li concentrations and isotopic compositions for all rock and mineral samples are plotted in Fig. 3. Table 1 reports data for simple pegmatites and the Harney Peak Granite, Table 2 for mineral separates and whole rock samples from the Tin Mountain pegmatite, Table 3 for fluid inclusions in quartz from the Tin Mountain pegmatite and Table 4 for the country rocks: quartz mica schists and Archean granites. Major, trace element and isotopic data (Sr, Nd, Pb and O) of these rock and mineral samples were

reported in Walker et al. (1986a; 1986b; 1989), Krogstad et al (1993) and Nabelek et al. (1992a; 1992b).

4.1. Lithium concentration and isotopic composition of granites and schists

The δ^7Li values for 25 Harney Peak Granite samples range from –3.1 to +6.6, with Li concentration ranging from 10 to 205 ppm. These concentrations are similar to values previously reported (8 to 171 ppm, Shearer et al, 1987a). In contrast to the distinct oxygen isotopic difference observed between biotite granites and tourmaline granites (Nabelek et al., 1992b), Li isotopic compositions are indistinguishable between these two types of granites (Fig. 4a) and show no correlation with Nd isotopes. Archean granite samples (Little Elk granite and Bear Mountain granite) have δ^7Li values within the range of the Harney Peak Granite, but with lower Li concentrations (4.9 and 7.7 ppm). Four simple pegmatites have the lowest Li concentrations of the granitic rocks (3 to 7.5 ppm), with δ^7Li ranging from +1.4 to +7.3. The δ^7Li values of four quartz mica schists vary from –3.1 to +2.5, overlapping with those of the Harney Peak Granite. The Li concentration in these schists is ~ 70 ppm, except for one that is a factor of two higher (150 ppm).

4.2. Lithium concentration and isotopic composition of Tin Mountain pegmatite

Three wall-zone whole-rock samples of the Tin Mountain pegmatite have Li concentrations ranging from 450 ppm to 735 ppm, two to 100 times higher than Harney

Peak Granite (4.9 to 205 ppm). Compared with the same minerals from granites (Bea et al., 1994; Neves, 1997; Pereira and Shaw, 1996), Li concentrations in minerals from all zones of the Tin Mountain pegmatite are also extremely high. Quartz has Li concentration ranging from 33 ppm to 135 ppm, while spodumene, muscovite and plagioclase have higher Li concentrations, decreasing in the order: spodumene (~3.7 wt%), muscovite (0.2 to 2.0 wt.%), plagioclase (100-1100 ppm) (Fig. 5a). The Li isotopic composition of these pegmatite samples is quite heavy. The three composite "whole-rock" samples from the wall zone have δ^7Li values ranging from +7.5 to +11.1, consistently heavier than Harney Peak Granite (Fig. 3). From the wall zone to the core, plagioclase, muscovite and spodumene display a narrow range in δ^7Li from +7.9 to +11.4, with resolvable systematic differences between minerals, whereas quartz displays a much larger range, from +14.7 to +21.3 (Fig. 5b), has systematically heavier δ^7Li values than coexisting minerals, and Li concentration inversely correlates with δ^7Li (Fig. 3). Fluid inclusions in quartz from all zones have much higher Li contents (283 to 3958 ppm) and lower δ^7Li values (+8.1 to +13.4) than bulk quartz (+14.7 to +21.3) but have δ^7Li similar to that of other minerals (+7.9 to +11.4) (Fig. 5). Compared with previously published δ^7Li for these samples (Tomascak et al., 1995), quartz and plagioclase measured here have similar values while muscovite is ~8‰ lighter than those previously reported. The reason for the discrepancy is unknown.

5. Discussion

Granites and granitic pegmatites are commonly found in spatial association and may be genetically related to each other, with pegmatites potentially representing the

final differentiation products of an evolving granite magmatic system. Study of the Harney Peak Granite, Tin Mountain pegmatite and associated potential source rocks thus provide a means with which to determine how Li isotopes fractionate during crustal melting and granite differentiation.

5.1. Lithium isotopic fractionation during granite petrogenesis

The amount by which Li isotopes fractionate during igneous differentiation is not fully understood. Tomascak et al. (1999) measured the Li isotopic composition of the crystallizing basalts of the Kilauea Iki lava lake, for which crystallization temperatures of 1050 ^{o}C to 1216^{o}C are well established. These investigators found no detectable Li isotopic fractionation within uncertainties of the measurement (±1.1‰, 2σ). Small Li isotopic fractionation (~ 3.5‰) is observed between olivine and pyroxenes at ~ 950 ^{o}C in peridotites, which is barely beyond the analytical uncertainty (±1.2‰, 2σ) (Seitz et al., 2004). Collectively, these studies suggest the amount of Li isotope fractionation at mantle temperatures is insignificant.

In contrast to the high temperatures and rapid crystallization and cooling experienced in dry, basaltic melts, granite is typically generated at lower temperatures (750-850 ^{o}C) by fluid-absent melting of crustal materials (Chappell et al., 2000), which is often followed by fractional crystallization, exsolution of a vapor phase and slow cooling. Each of these processes (partial melting, fractional crystallization, fluid exsolution, cooling) could, in principle, produce isotopic fractionation. Below we explore the general factors that influence Li concentration and isotopic composition in granitic systems, and

then explore what new insights the data from the Harney Peak Granite and Tin Mountain pegmatite provide.

5.1.1. Lithium isotopic fractionation during crystal-melt equilibria

5.1.1.1. Theoretical considerations

Lithium concentrations in granites are controlled by bulk partition coefficients between melt and solid, which vary with the compositions of both minerals and melts. Lithium in S-type granites is mainly contained within micas (biotite and muscovite), with lesser amounts in cordierite (Bea et al., 1994; Neves, 1997; Pereira and Shaw, 1996). Experimental studies of Li partitioning between biotite, muscovite, cordierite and coexisting peraluminous silicic melt show that Li is slightly compatible in biotite ($D_{Li}^{Bt/melt}$ ranges from 1.0-1.7, and decreases with increasing temperature) and is incompatible in muscovite ($D_{Li}^{Ms/melt} \sim 0.8$) and cordierite ($D_{Li}^{Crd/melt}$ ranges from 0.44 to 0.12, decreasing with increasing temperature) (Evensen and London, 2003; Icenhower and London, 1995). Collectively, these studies suggest that Li behaves as a moderately incompatible element during granite differentiation, and Li concentrations are thus expected to decrease with the degree of melting and increase with progressive crystal fractionation.

Lithium isotope fractionation between minerals and melt is governed by the general rules of stable isotope fractionation. As discussed in Chacko et al. (2001), equilibrium isotope fractionation is due to differences in zero point energy (ΔZPE) between molecules with different isotopes. Substances with larger ΔZPE during isotope

substitution favor the heavier isotope. Since substances with stronger bonds will have larger ΔZPE during isotope substitution, heavy isotopes, therefore, will favor substances with stronger bonds or higher energy sites. Lithium is monovalent (1^+) and, hence, not redox sensitive. In addition, Li, like B and other light cations, is bonded to oxygen in most silicates (Wenger and Armbruster, 1991), and isotopic fractionation in silicates is controlled strictly by the relative site energies at the same temperature. In most solids, Li occupies either tetrahedrally- or octahedrally- coordinated sites and potential energies in the polyhedra generally decrease with increasing coordination numbers (Wenger and Armbruster, 1991). Therefore, substances with tetrahedrally coordinated Li are expected to prefer heavy Li isotopes to those where Li is octahedrally coordinated. This can only be considered as a rather general guide since Li coordination polyhedra are more or less distorted in most minerals due to its small ionic radius and lower charge and hence the potential energies can be largely changed and overlapping.

Lithium enters two- and four-fold coordinated interstitial sites in quartz (Sartbaeva et al., 2004), but the concentration in quartz is typically low, so quartz is not expected to exert a major control on isotopic fractionation in granites. In the most Li-rich minerals, Li is octahedrally coordinated e.g., spodumene (Clarke and Spink, 1969; Li and Peacor, 1968), micas (Brigatti et al., 2000; 2003; Robert et al., 1983), and cordierite (Bertoldi et al., 2004). In contrast, Li is tetrahedrally coordinated in granitic melts (Soltay and Henderson, 2005a; 2005b; Zhao et al., 1998). At low temperatures, these different coordination numbers for Li between melts and crystals may produce measurable Li isotopic fractionation. Based on the above considerations, the most important Li-bearing minerals (e.g., micas, spodumene) are expected to be isotopically lighter than coexisting

melts. If the fractionation or differentiation is large enough, granitic melts should evolve to isotopically heavier δ^7Li values with differentiation (Fig. 6a).

5.1.1.2. Observations from the Harney Peak Granite

The Harney Peak Granite was likely produced by melting sediments derived from Archean granites and surrounding Proterozoic schists (Krogstad et al., 1993; Nabelek et al., 1992a; 1992b; Walker et al., 1986a; 1989). Both of these potential source rocks have experienced different grades of regional metamorphism and schists near the Harney Peak Granite and related pegmatites have been metasomatized and show elevated Li concentrations and highly variable δ^7Li values (Teng et al., 2006a; Wilke et al., 2002). However, the similar Li and δ^7Li values between Archean granites and Proterozoic schists studied here and typical schists, unmetamorphosed shales and granites worldwide (Teng et al., 2004a; 2006b) suggest that any metasomatic and/or metamorphic effects on the Li concentration and δ^7Li in the South Dakota samples has been small. Therefore, these samples can be considered as representative of the potential source rocks of the Harney Peak Granite.

The δ^7Li values of most Harney Peak Granites (22 out of 25) lie within the range observed in Archean granites and Proterozoic schists (Fig. 3) and show no correlation with the degree of differentiation, as inferred from various compositional parameters (e.g., SiO_2, Li, Rb contents) (Fig. 4). These observations, together with the identical δ^7Li value of the metasedimentary rock WC-4 and its inferred *in situ* melt (pegmatitic vein WC-9), indicate that the δ^7Li values of the Harney Peak Granites are mainly controlled by their source rocks and are not strongly affected by crustal anatexis and granite crystallization.

This conclusion is consistent with previous granite studies. Thirteen S-type granites from Australia, covering a large range of compositions, display a very limited range in δ^7Li values (-1.4 to +2.8), which is similar to that observed in their presumed protoliths (Bryant et al., 2004; Teng et al., 2004a). The δ^7Li values of I-type granites from Australia show larger variations (+1.9 to +8.1) and correlate with inferred differences in source rocks. These variations do not correlate with the degree of granite differentiation (Bryant et al., 2004; Teng et al., 2004a).

The origin of the three isotopically heavier (δ^7Li = +5.5 to +6.6) Harney Peak Granite samples is uncertain. One of them (HP30A) has elevated δD, which may reflect interactions with isotopically heavy H_2O derived from metamorphic dehydration of country rocks (Nabelek et al., 1992b). Alternatively, these three granites may reflect extensive, local crystal-melt fractionation, since one of them has the highest Sr and Ba contents and also has high Rb content.

5.1.2. Lithium isotopic fractionation during fluid-melt equilibria

5.1.2.1. Theoretical considerations

Compared with Li partitioning between minerals and melt, there is a considerable range in Li partition coefficients between supercritical fluids and melts (Candela and Piccoli, 1995). The most important factors controlling Li partitioning between fluid and melt are fluid composition and temperature. For example, in peraluminous granite-pegmatite systems, $D_{Li}^{fluid/melt}$ is ~ 0.4 and does not change within a temperature interval of 650-775 ^oC at 200 MPa (London et al., 1988). In a metaluminous system at similar

temperatures and pressures (i.e., 800 ^{o}C and 200 MPa), but with a much higher Cl content, Webster et al. (1989) found higher $D_{Li}^{fluid/melt}$, which increases from 1.1 to 2.5 as the Cl content of the vapor doubles. In addition, Webster et al (1989) reported that partition coefficients between fluid and melt also increase with temperature and the mole fraction of water present in the fluids.

Lithium in supercritical fluids bonds with Cl to form LiCl (Candela and Piccoli, 1995). In granitic melts, Li bonds with O (Soltay and Henderson, 2005a; 2005b; Zhao et al., 1998). These different types of bonds (ionic vs. covalent) make it difficult to use the difference of Li coordination to predict the isotopic fractionation between these two phases. To date, no experiment has measured the Li isotopic fractionation factor between supercritical fluids and melts. Recent experimental studies on supercritical fluids and minerals show conflicting results. Lynton et al. (2005) studied Li isotopic fractionation between quartz, muscovite and hydrothermal fluid and found that fluids are isotopically lighter than minerals. In contrast, Wunder et al., (2006) investigated Li isotopic fractionation between synthetic spodumene and hydrothermal fluid and observed a temperature-dependent fractionation, with fluids heavier than coexisting spodumene. The latter study agrees with a few empirical studies on Li isotopic compositions of hydrothermal fluids and altered basalts, which suggest that fluids are isotopically heavier than basalts (Chan et al., 1993; 1994; Foustoukos et al., 2004). The cause of the difference between these studies remains unknown. If there is Li isotopic fractionation during the process of supercritical fluid separation from granitic melts, the minerals crystallized from the fluids would have different Li isotopic compositions than those formed from the melts, with the difference depending on the Li isotopic fractionation

factor between fluid and melt (α). For conditions where α is 1.004, $D_{Li}^{fluid/melt} \leq 2.5$ (the maximum value at 800^{o}C, 200MPa with 6.13M Cl in fluid, Webster et al., 1989) and the fraction of fluids exsolved (F) $\leq$ 14% (the maximum concentration of H_2O at saturation in peraluminous melt, London et al., 1988), the isotopic compositions of both residual melts and exsolved fluids change little with progressive fluid exsolution (assuming Rayleigh distillation as an extreme process) (Fig. 6b).

This calculation shows that fluid exsolution should have minimal effect on Li isotopic composition of granites that exsolve modest quantity of water. However, if a large amount of fluids exsolve and is released from the system (i.e., F is large), at relatively low temperature (i.e., α is large), then fluid exsolution may influence the Li isotopic compositions of granitic systems. Minerals that crystallize from exsolved fluids, fluid-rich melts or re-equilibrated with late fluids at subsolidus conditions should be isotopically heavier than those that crystallize from melts only, assuming that fluids are isotopically heavier than melts.

5.1.2.2. Observations from the Tin Mountain pegmatite

The source of the Tin Mountain pegmatite melt can be either the surrounding metasediments or the Harney Peak Granite. In order to produce the highly zoned pegmatite, melts derived from these potential sources must experience extensive crystal-melt fractionation (Walker et al., 1986b). If Li isotopes fractionate during this process, then the extensive crystal-melt fractionation (i.e., large F) could potentially shift the isotopic composition of the melt (Fig. 6a). In this case, the extremely fractionated Tin Mountain pegmatite should be isotopically heavier than the Harney Peak Granite or

schists. A plot of δ^7Li vs. Rb for the Harney Peak Granite, simple pegmatites and Tin Mountain pegmatite shows that highly fractionated samples (e.g., pegmatites with Rb >200 ppm) have heavier Li isotopic compositions compared to moderately fractionated granites (e.g., granites and pegmatites with Rb <200 ppm) and schists (Fig. 7). This observation supports the idea that significant isotopic fractionation during crystal-melt fractionation only occurs during the latest stages of granite differentiation at relatively low temperatures.

In addition to extensive crystal-fractionation, increased H_2O contents may have played a role in producing the isotopically heavy Tin Mountain pegmatite. Previous studies suggest that most parts of the Tin Mountain pegmatite crystallized from coexisting fluid and melt, as indicated by the kinked chondrite-normalized REE patterns in apatites (Walker et al., 1986b) (the tetrad effect, Peppard et al., 1969), which normally occurs during late-stage granite evolution, where REEs partition between melt and coexisting, compositionally complicated fluids (Jahn et al., 2001). The presence of a fluid phase is further supported by the fact that both fluid and melt inclusions occur in quartz from all zones of the Tin Mountain pegmatite (Sirbescu and Nabelek, 2003a; 2003b). Two of the three whole rocks from the wall zone studied here (samples 10-3 and 43-1) show the tetrad effect, and they are isotopically heavier than the one without the tetrad effect (sample 9-2). This may indicate that a fluid phase exsolved during crystallization of the wall zone, and that all later zones, including part of the wall zone, crystallizing from a mixed fluid-melt phase. If true, then the ~4‰ difference in δ^7Li values between the wall zone sample 9-2 (Table 2) and fluid inclusions (Table 3) may reflect the Li isotopic fractionation during fluid exsolution (i.e., fluid-melt fractionation). This amount

of fractionation is consistent with results from previous studies on hydrothermal alteration of basalts (Chan et al., 1993; 1994; Foustoukos et al., 2004).

5.2. Lithium isotopic fractionation within the Tin Mountain pegmatite

Intra-mineral isotopic fractionation is important for understanding both Li isotopic systematics and potentially using Li isotopes for thermometry. The Li-enriched Tin Mountain pegmatite crystallized at relatively low temperatures (Sirbescu and Nabelek, 2003a; 2003b; Walker et al., 1986b), so Li isotope fractionation may be dramatic.

The δ^7Li of quartz is different from that of all other minerals examined from the Tin Mountain pegmatite. Quartz shows a relatively large range in δ^7Li from +14.7 to +21.3, and δ^7Li correlates negatively with Li concentration (Fig. 8). This quartz contains both primary and secondary fluid inclusions, which are highly enriched in Li (Table 3). The negative correlation for quartz may reflect mixing between isotopically heavy quartz and lighter fluid inclusions. Extrapolating from this trend, the inclusion-free quartz is expected to have a relatively low Li concentration ($\leq$ 30 ppm) and heavy Li isotopic composition ($\geq$ +21). This agrees with the only available Li isotopic data for fluid inclusion-free quartz (from a Li-rich granitic pegmatite), which has δ^7Li = +27 ± 2 and 17 ppm Li (Lynton et al., 2005). The fluid inclusions should be Li-rich ($\geq$140 ppm) and isotopically lighter ($\leq$+15). This agrees with our isotopic study on fluid inclusions. Fluid inclusions in eight quartz samples from the Tin Mountain pegmatite have high Li contents (283 to 3958 ppm) and lighter δ^7Li values, ranging from +8.1 to +13.4 (Table 3).

This range is similar to that observed in the other pegmatite minerals, but is considerably lighter than quartz.

The intra-mineral isotopic fractionation between quartz and other minerals may result from equilibrium isotopic fractionation during crystallization and may reflect the preference of quartz for heavy Li. As discussed previously, Li enters quartz in two- or four-fold sites, whereas for other minerals Li is octahedrally coordinated (see section 5.1.1.1).

The data collected here are consistent with observations from Wunder et al. (2006) but different from those recently reported by Lynton et al (2005) in several important ways. Lynton et al (2005) found that at 500 ^{o}C, muscovite is 9‰ heavier than quartz, which, in turn, is 10‰ heavier than fluids. Moreover, they observed that Li isotopic fractionation between minerals (muscovite/quartz) and fluids depends on the Li concentration in the fluids and reduces to ~10‰ when Li concentration in fluids increases. Finally, they found that Li isotopic fractionation between quartz and fluids decreases from 10‰ to 5‰ when the temperature of the experiment decreases from 500 to 400 ^{o}C. These observations contradict the general theory of isotope fractionation that the isotopic fractionation factor should decrease with increasing temperature and be independent of element concentrations of phases (Chacko et al., 2001). Clearly, more studies are needed to fully understand the cause of these differences.

6. Conclusions

1. The Harney Peak Granite has δ^{7}Li ranging from -3.1 to +6.6, with most falling within the range defined by their Archean and Proterozoic potential sources (-3.1

to +2.5). There is no correlation between δ^7Li and geochemical indicators of granitic differentiation, suggesting that the Li isotopic compositions of the granite mainly reflect those of their sources.

2. Three bulk rocks from the wall zone provide the best estimate of the bulk composition of the Tin Mountain pegmatite. Their average δ^7Li of +9.9 is much heavier than that of the Harney Peak Granite. This isotopically heavy signature results from extensive crystal fractionation and agrees with the predicated behavior of Li during extensive Rayleigh fractionation. The pegmatite data, compared with the data from the Harney Peak Granite, suggest that both crystal-melt and fluid-melt fractionation during granite differentiation can affect the Li isotopic compositions of highly fractionated granites, but does not play an important role in low to moderately fractionated granites.
3. All minerals from the Tin Mountain pegmatite have high Li concentrations and similar δ^7Li values (+7.9 to +11.4), except quartz. Quartz is less enriched in Li, is ~ 6-11‰ heavier than all other minerals, and displays a negative correlation between δ^7Li and Li concentration. This correlation reflects a mixture between heavy Li bonded in inclusion-free quartz (> +21) and lighter, Li-rich fluid inclusions (+8.1 to +13.4). The large difference in isotopic composition between quartz and other minerals probably reflects equilibrium Li isotopic fractionation, with heavy Li preferring low-coordination sites (quartz) to more highly coordinated ones.

Acknowledgements

We thank Boz Wing and James Farquhar for discussions, Fuyuan Wu and Paul Tomascak for comments on an earlier draft, and Grant Henderson for sharing work in progress. Peter Nabelek and Ted Labotka are thanked for their very constructive comments, which greatly improved the manuscript. FZT appreciates helpful discussions with Paul Tomascak about initializing this project, as well as the efforts of Dr. Richard Ash in the Plasma Lab. This work was supported by the N.S.F (EAR 0208012).

References

Bea, F., Pereira, M.D., and Stroh, A. (1994) Mineral leucosome trace-element partitioning in a peraluminous migmatite (a Laser Ablation-ICP-MS Study). Chemical Geology, 117(1-4), 291-312.

Belshaw, N.S., Freedman, P.A., O'Nions, R.K., Frank, M., and Guo, Y. (1998) A new variable dispersion double-focusing plasma mass spectrometer with performance illustrated for Pb isotopes. International Journal of Mass Spectrometry, 181, 51-58.

Benton, L.D., Ryan, J.G., and Savov, I.P. (2004) Lithium abundance and isotope systematics of forearc serpentinites, Conical Seamount, Mariana forearc: Insights into the mechanics of slab-mantle exchange during subduction. Geochemistry Geophysics Geosystems, 5, Q08J12, doi:10.1029/2004GC000708.

Bertoldi, C., Proyer, A., Garbe-Schonberg, D., Behrens, H., and Dachs, E. (2004) Comprehensive chemical analyses of natural cordierites: implications for exchange mechanisms. Lithos, 78(4), 389-409.

Bottrell, S.H., Yardley, B., and Buckley, F. (1988) A modified crush-leach method for the analysis of fluid inclusion electrolytes. Bullétin de Minéralogie, 111, 272-290.

Bouman, C., Elliott, T., and Vroon, P.Z. (2004) Lithium inputs to subduction zones. Chemical Geology, 212(1-2), 59-79.

Brigatti, M.F., Lugli, C., Poppi, L., Foord, E.E., and Kile, D.E. (2000) Crystal chemical variations in Li- and Fe-rich micas from Pikes Peak batholith (central Colorado). American Mineralogist, 85(9), 1275-1286.

Brigatti, M.F., Kile, D.E., and Poppi, L. (2003) Crystal structure and chemistry of lithium-bearing trioctahedral micas-3T. European Journal of Mineralogy, 15(2), 349-355.

Bryant, C.J., Chappell, B.W., Bennett, V.C., and McCulloch, M.T. (2004) Lithium isotopic composition of the New England Batholith: correlations with inferred source rock compositions. Transactions of the Royal Society of Edinburgh-Earth Sciences, 95, 199-214.

Candela, P.A., and Piccoli, P.M. (1995) Model ore-metal partitioning from melts into vapor and vapor/brine mixtures. In J.F.H. Thompson, Ed. Granites, Fluids, and Ore Deposits, 23, p. 101-128. Mineralogical Association of Canada.

Chacko, T., Cole, D.R., and Horita, J. (2001) Equilibrium oxygen, hydrogen and carbon isotope fractionation factors applicable to geological systems. In J.W. Valley, and D.R. Cole, Eds. Stable isotope geochemistry, 43, p. 1-82. Mineralogical Society of America, Washington, DC.

Chan, L.-H., and Kastner, M. (2000) Lithium isotopic compositions of pore fluids and sediments in the Costa Rica subduction zone: implications for fluid processes and

sediment contribution to the arc volcanoes. Earth and Planetary Science Letters, 183(1-2), 275-290.

Chan, L.H., Edmond, J.M., Thompson, G., and Gillis, K. (1992) Lithium isotopic composition of submarine basalts: implications for the lithium cycle in the oceans. Earth and Planetary Science Letters, 108(1-3), 151-160.

Chan, L.H., Edmond, J.M., and Thompson, G. (1993) A lithium isotope study of hot-springs and metabasalts from Mid-Ocean ridge hydrothermal systems. Journal of Geophysical Research-Solid Earth, 98(B6), 9653-9659.

Chan, L.H., Gieskes, J.M., You, C.F., and Edmond, J.M. (1994) Lithium isotope geochemistry of sediments and hydrothermal fluids of the Guaymas Basin, Gulf of California. Geochimica et Cosmochimica Acta, 58(20), 4443-4454.

Chan, L.H., Alt, J.C., and Teagle, D.A.H. (2002) Lithium and lithium isotope profiles through the upper oceanic crust: a study of seawater-basalt exchange at ODP Sites 504B and 896A. Earth and Planetary Science Letters, 201(1), 187-201.

Chan, L.H. (2004) Mass spectrometric techniques for the determination of lithium isotopic composition in geological material. In P.A. De Groot, Ed. Handbook of Stable Isotope Analytical Techniques, 1, p. 122-141. Elsevier.

Chappell, B.W., White, A.J.R., Williams, I.S., Wyborn, D., and Wyborn, L.A.I. (2000) Lachlan Fold Belt granites revisited: high- and low-temperature granites and their implications. Australian Journal of Earth Sciences, 47(1), 123-138.

Clarke, P.T., and Spink, J.M. (1969) Crystal structure of β spodumene, $LiAlSi_2O_6$-II. Zeitschrift Fur Kristallographie Kristallgeometrie Kristallphysik Kristallchemie, 130(4-6), 420.

Duke, E.F., Shearer, C.K., Redden, J.A., and Papike, J.J. (1990) Proterozoic granite-pegmatite magmatism, Black Hills, South Dakota: Structure and geochemical zonation. In J.F. Lewry, and M.R. Stauffer, Eds. Tthe Trans-Hudson Orogen, p. 253-269. Geol. Assoc. Canda Spec. Paper 37.

Elliott, T., Jeffcoate, A.B., and Bouman, C. (2004) The terrestrial Li isotope cycle: light-weight constrains on mantle convection. Earth and Planetary Science Letters, 220, 231-245.

Evensen, J.M., and London, D. (2003) Experimental partitioning of Be, Cs, and other trace elements between cordierite and felsic melt, and the chemical signature of S-type granite. Contributions to Mineralogy and Petrology, 144(6), 739-757.

Flesch, G.D., Anderson, A.R.J., and Svec, H.J. (1973) A secondary isotopic standard for $^{6}Li/^{7}Li$ determinations. Int. J. Mass Spectrom. Ion Proc., 12(265-272).

Foustoukos, D.I., James, R.H., Berndt, M.E., and Seyfried, J., W.E. (2004) Lithium isotopic systematics of hydrothermal vent fluids at the Main Endeavour Field, Northern Juan de Fuca Ridge. Chemical Geology, 212(1-2), 17-26.

Huh, Y., Chan, L.H., and Chadwick, O.A. (2004) Behavior of lithium and its isotopes during weathering of Hawaiian basalt. Geochemistry Geophysics Geosystems, 5(9), Q09002, doi:10.1029/2004GC000729.

Icenhower, J., and London, D. (1995) An experimental study of element partitioning among biotite, muscovite, and coexisting peraluminous silicic melt at 200 MPa (H_2O). American Mineralogist, 80(11-12), 1229-1251.

Jahn, B.M., Wu, F.Y., Capdevila, R., Martineau, F., Zhao, Z.H., and Wang, Y.X. (2001) Highly evolved juvenile granites with tetrad REE patterns: the Woduhe and

Baerzhe granites from the Great Xing'an Mountains in NE China. Lithos, 59(4), 171-198.

James, R.H., Allen, D.E., and Seyfried, W.E., Jr. (2003) An experimental study of alteration of oceanic crust and terrigenous sediments at moderate temperatures (51 to 350 ^{o}C): Insights as to chemical processes in near-shore ridge-flank hydrothermal systems. Geochimica et Cosmochimica Acta, 67(4), 681-691.

Kisakurek, B., Widdowson, M., and James, R.H. (2004) Behaviour of Li isotopes during continental weathering: The Bidar laterite profile, India. Chemical Geology, 212(1-2), 27-44.

Krogstad, E.J., Walker, R.J., Nabelek, P.I., and Russnabelek, C. (1993) Lead isotopic evidence for mixed sources of Proterozoic granites and pegmatites, Black-Hills, South-Dakota, USA. Geochimica et Cosmochimica Acta, 57(19), 4677-4685.

Krogstad, E.J., and Walker, R.J. (1996) Evidence of heterogeneous crustal sources: The Harney peak granite, South Dakota, USA. Transactions of the Royal Society of Edinburgh-Earth Sciences, 87, 331-337.

Li, C.T., and Peacor, D.R. (1968) Crystal structure of $LiAlSi_2O_6$-2 (β Spodumene). Zeitschrift Fur Kristallographie Kristallgeometrie Kristallphysik Kristallchemie, 126(1-3), 46.

London, D., Hervig, R.L., and Morgan, G.B. (1988) Melt-vapor solubilities and elemental partitioning in peraluminous granite-pegmatite systems - experimental results with Macusani Glass at 200 MPa. Contributions to Mineralogy and Petrology, 99(3), 360-373.

Lundstrom, C.C., Chaussidon, M., Hsui, A.T., Kelemen, P., and Zimmerman, M. (2005) Observations of Li isotopic variations in the Trinity Ophiolite: Evidence for isotopic fractionation by diffusion during mantle melting. Geochimica et Cosmochimica Acta, 69(3), 735-751.

Lynton, S.J., Walker, R.J., and Candela, P.A. (2005) Lithium isotopes in the system Qz-Ms-fluid:An experimental study. Geochimica et Cosmochimica Acta, 69(13), 3337-3347.

Moriguti, T., and Nakamura, E. (1998) High-yield lithium separation and the precise isotopic analysis for natural rock and aqueous samples. Chemical Geology, 145(1-2), 91-104.

Nabelek, P.I., Russ-Nabelek, C., and Denison, J.R. (1992a) The generation and crystallization conditions of the Proterozoic Harney Peak leukogranite, Black Hills, South-Dakota, USA - petrologic and geochemical constraints. Contributions to Mineralogy and Petrology, 110(2-3), 173-191.

Nabelek, P.I., Russ-Nabelek, C., and Haeussler, G.T. (1992b) Stable isotope evidence for the petrogenesis and fluid evolution in the Proterozoic Harney Peak leukogranite, Black-Hills, South-Dakota. Geochimica et Cosmochimica Acta, 56(1), 403-417.

Nabelek, P.I., and Bartlett, C.D. (1998) Petrologic and geochemical links between the post-collisional Proterozoic Harney Peak leucogranite, South Dakota, USA, and its source rocks. Lithos, 45(1-4), 71-85.

Neves, L. (1997) Trace element content and partitioning between biotite and muscovite of granitic rocks: a study in the Viseu region (Central Portugal). European Journal of Mineralogy, 9(4), 849-857.

Norton, J.J., and Redden, J.A. (1990) Relations of zoned pegmatites to other pegmatites, granite, and metamorphic rocks in the southern Black Hills, South Dakota. American Mineralogist, 75, 631-655.

Peppard, D.F., Mason, G.W., and Lewey, S. (1969) A tetrad effect in liquid-liquid extraction ordering of lanthanides(3). Journal of Inorganic & Nuclear Chemistry, 31(7), 2271-&.

Pereira, M.D., and Shaw, D.M. (1996) B and Li distribution in the Pena Negra complex: An alpha-track study. American Mineralogist, 81(1-2), 141-145.

Pistiner, J.S., and Henderson, G.M. (2003) Lithium-isotope fractionation during continental weathering processes. Earth and Planetary Science Letters, 214(1-2), 327-339.

Qi, H.P., Taylor, P.D.P., Berglund, M., and De Bievre, P. (1997) Calibrated measurements of the isotopic composition and atomic weight of the natural Li isotopic reference material IRMM-016. International Journal of Mass Spectrometry, 171(1-3), 263-268.

Ratte, J.C., and Zartman, R.E. (1975) Bear Mountain gneiss dome, Black Hills, South Dakota. Geol. Surv. Amer. Abstr. Progs., 2(5), 345.

Redden, J.A., Norton, J.J., and McLaughlin, R.J. (1985) Geology of the Harney Peak granite, Black Hills, South Dakota. In F.J. Rich, Ed. Geology of the Black Hills, South Dakota and Wyoming, p. 225-240. Amer. Geol. Inst.

Richter, F.M., Davis, A.M., DePaolo, D.J., and Watson, E.B. (2003) Isotope fractionation by chemical diffusion between molten basalt and rhyolite. Geochimica et Cosmochimica Acta, 67(20), 3905-3923.

Robert, J.L., Volfinger, M., Barrandon, J.N., and Basutcu, M. (1983) Lithium in the interlayer space of synthetic trioctahedral micas. Chemical Geology, 40(3-4), 337-351.

Rudnick, R.L., Tomascak, P.B., Njo, H.B., and Gardner, L.R. (2004) Extreme lithium isotopic fractionation during continental weathering revealed in saprolites from South Carolina. Chemical Geology, 212(1-2), 45-57.

Sartbaeva, A., Wells, S.A., and Redfern, S.A.T. (2004) Li^+ ion motion in quartz and beta-eucryptite studied by dielectric spectroscopy and atomistic simulations. Journal of Physics-Condensed Matter, 16(46), 8173-8189.

Seitz, H.-M., Brey, G.P., Lahaye, Y., Durali, S., and Weyer, S. (2004) Lithium isotopic signatures of peridotite xenoliths and isotopic fractionation at high temperature between olivine and pyroxenes. Chemical Geology, 212(1-2), 163-177.

Seyfried Jr., W.E., Chen, X., and Chan, L.-H. (1998) Trace element mobility and lithium isotope exchange during hydrothermal alteration of seafloor weathered basalt: An experimental study at 350 ^{o}C, 500 bars. Geochimica et Cosmochimica Acta, 62(6), 949-960.

Shearer, C.K., Papike, J.J., and Laul, J.C. (1987a) Mineralogical and chemical evolution of a rare-element granite-pegmatite system - Harney Peak Granite, Black Hills, South-Dakota. Geochimica et Cosmochimica Acta, 51(3), 473-486.

Shearer, C.K., Papike, J.J., Redden, J.A., Simon, S.B., Walker, R.J., and Laul, J.C. (1987b) Origin of pegmatitic granite segregations, Willow Creek, Black Hills, South-Dakota. Canadian Mineralogist, 25, 159-171.

Sirbescu, M.L.C., and Nabelek, P.I. (2003a) Crustal melts below 400 ^{o}C. Geology, 31(8), 685-688.

-. (2003b) Crystallization conditions and evolution of magmatic fluids in the Harney Peak Granite and associated pegmatites, Black Hills, South Dakota - Evidence from fluid inclusions. Geochimica et Cosmochimica Acta, 67(13), 2443-2465.

Soltay, L.G., and Henderson, G.S. (2005a) Structural differences between lithium silicate and lithium germanate glasses by Raman spectroscopy. Physics and Chemistry of Glasses, 46(4), 381-384.

-. (2005b) The structure of lithium containing silicate and germanate glasses. Canadian Mineralogist, 43, 1643-1651.

Teng, F.-Z., McDonough, W.F., Rudnick, R.L., Dalpe, C., Tomascak, P.B., Chappell, B.W., and Gao, S. (2004a) Lithium isotopic composition and concentration of the upper continental crust. Geochimica et Cosmochimica Acta, 68(20), 4181-4192.

Teng, F.-Z., McDonough, W.F., Rudnick, R.L., and Gao, S. (2004b) Lithium isotopic composition of the deep continental crust. EOS 85 (47), Abstr. V51C-0597.

Teng, F.-Z., McDonough, W.F., Rudnick, R.L., and Walker, R.J. (2006a) Diffusion-driven extreme lithium isotopic fractionation in country rocks of the Tin Mountain pegmatite. Earth and Planetary Science Letters, 243(3-4), 701-710.

Teng, F.-Z., McDonough, W.F., Rudnick, R.L., and Wing, B.A. (2006b) Lack of lithium isotopic fractionation during progressive metamorphic dehydration in metapelite: A case study from the Onawa contact aureole, Maine. Chemical Geology, in review

Tomascak, P.B., Lynton, S.J., Walker, R.J., and E.J., K. (1995) Li isotope geochemistry of the Tin Mountain pegmatite, Black Hills, South Dakota. In: The Origin of Granites and related Rocks. Brown. M, Piccoli PM (eds) US Geol Surv Circ 1129: 151-152.

Tomascak, P.B., Tera, F., Helz, R.T., and Walker, R.J. (1999) The absence of lithium isotope fractionation during basalt differentiation: New measurements by multicollector sector ICP- MS. Geochimica et Cosmochimica Acta, 63(6), 907-910.

Tomascak, P.B. (2004) Developments in the understanding and application of lithium isotopes in the Earth and planetary sciences. In C. Johnson, B. Beard, and F. Albarede, Eds. Geochemistry of non-traditional stable isotopes, 55, p. 153-195. Mineralogical Society of America, Washington, DC.

Walker, R.J., Hanson, G.N., Papike, J.J., and O'Neil, J.R. (1986a) Nd, O and Sr isotopic constraints on the origin of Precambrian rocks, Southern-Black-Hills, South-Dakota. Geochimica et Cosmochimica Acta, 50(12), 2833-2846.

Walker, R.J., Hanson, G.N., Papike, J.J., O'Neil, J.R., and Laul, J.C. (1986b) Internal evolution of the Tin Mountain Pegmatite, Black Hills, South-Dakota. American Mineralogist, 71(3-4), 440-459.

Walker, R.J., Hanson, G.N., and Papike, J.J. (1989) Trace-element constraints on pegmatite genesis - Tin Mountain Pegmatite, Black Hills, South-Dakota. Contributions to Mineralogy and Petrology, 101(3), 290-300.

Webster, J.D., Holloway, J.R., and Hervig, R.L. (1989) Partitioning of lithophile trace-elements between H_2O and $H_2O + CO_2$ fluids and topaz rhyolite melt. Economic Geology, 84(1), 116-134.

Wenger, M., and Armbruster, T. (1991) Crystal-chemistry of lithium - oxygen coordination and bonding. European Journal of Mineralogy, 3(2), 387-399.

Wilke, M., Nabelek, P.I., and Glascock, M.D. (2002) B and Li in Proterozoic metapelites from the Black Hills, USA: Implications for the origin of leucogranitic magmas. American Mineralogist, 87(4), 491-500.

Williams, L.B., and Hervig, R.L. (2005) Lithium and boron isotopes in illite-smectite: The importance of crystal size. Geochimica et Cosmochimica Acta, 69(24), 5705-5716.

Wunder, B., Meixner, A., Romer, R.L., and Heinrich, W. (2006) Temperature-dependent isotopic fractionation of lithium between clinopyroxene and high-pressure hydrous fluids. Contributions to Mineralogy and Petrology, 151(1), 112-120.

Zack, T., Tomascak, P.B., Rudnick, R.L., Dalpe, C., and McDonough, W.F. (2003) Extremely light Li in orogenic eclogites: The role of isotope fractionation during dehydration in subducted oceanic crust. Earth and Planetary Science Letters, 208(3-4), 279-290.

Zartman, R.E., Norton, J.J., and Stern, T.W. (1964) Ancient granite gneiss in the Black Hills, South Dakota. Science, 145, 479-481.

Zartman, R.E., and Stern, T.W. (1967) Isotopic age and geologic relationships of the Little Elk Granite, Northern Black Hills, South Dakota. U.S.G.S. Prof. Paper, 575D, 157-163.

Zhao, J., Gaskell, P.H., Cluckie, M.M., and Soper, A.K. (1998) A neutron diffraction, isotopic substitution study of the structure of $Li_2O.2SiO_2$ glass. Journal of Non-Crystalline Solids, 234, 721-727.

Table 1. Lithium isotopic composition and concentration of Harney Peak Granite and simple pegmatites from the Black Hills, South Dakota

Sample ID	$\delta^{7}Li$[1]	Li[2] (ppm)	$\delta^{18}O$[3]
Harney Peak Granite			
3-1B	+4.0	38	13.41
3-1B replicate[4]	+3.9		
4-1	+6.6	38	13.84
4-1 replicate	+6.2		
1-1	+2.1	86	12.88
2-1	+0.2	16	13.23
HP-3B	+1.6	205	13.69
HP-8 4L	+1.1	69	11.92
HP-8 8L	+0.0	30	11.78
HP-20	+2.9	43	10.94
HP-1	-3.1	26	14.08
HP-2	-2.1	9.7	13.34
HP-6	-1.5	12	12.41
HP-14	-1.4	31	12.76
HP2A	+2.2	14	13
HP10B	+0.3	178	12.9
HP13A	+2.2	103	11.9
HP13C	+2.3	103	12
HP14A	+2.0	86	10.8
HP17	-1.1	48	13
HP22	-0.1	23	11.9
HP24B	+3.9	37	12.7
HP30A	+5.5	60	12.3
HP39A	+6.6	20	13
HP43A	0	41	13
HP44A	+1.1	41	11.3
HP45B	+1.0	27	12.5
Simple pegmatite			
WC-9	+1.4	7.5	13.83
5-1	+3.9	5.1	13.36
6-3	+6.1	5.7	12.68
6-4	+7.3	3.0	11.59

1. Analytical uncertainty is < ± 1‰ (2σ), based on both pure Li solutions and natural rock standard (see text for details).
2. Lithium concentration measured by comparison of signal intensities with 50 or 100 ppb LSVEC.
3. Data from Walker et al (1986a; 1989) and (Nabelek et al., 1992a).
4. Replicate: repeat column chemistry from the same stock sample solution.

Table 2. Lithium isotopic composition and concentration of mineral and whole rock samples from the Tin Mountain pegmatite, Black Hills, South Dakota

Sample ID[1]	Zone	δ^7Li[2]	Li (ppm)[3]	$\delta^{18}O$[4]
		Quartz		
11-3A	Wall	+18.3	61	12.4
17-1C	2nd intermediate	+16.9	97	12.5
16-2C	3rd intermediate	+17.0	141	12.9
16-2C replicate[5]		+16.3	129	
16-10A	3rd intermediate	+14.7	92	12.5
16-10A replicate		+14.7	98	
18-2A	Core	+18.4	87	12.7
18-2A replicate		+17.7	79	
19-1A	Core	+19.3	47	12.5
19-1A replicate		+19.2	46	
15-1A	Fracture filling	+19.9	52	12.6
15-3A	Fracture filling	+21.3	33	12.8
		Plagioclase		
11-3C	Wall	+8.8	104	11
16-2D	3rd intermediate	+9.7	578	11.4
16-2D replicate		+8.9	587	
16-10B	3rd intermediate	+9.2	564	11.2
16-10Breplicate		+8.3	543	
19-1C	Core	+9.9	1098	11.3
19-1C replicate		+9.3	940	
		Li-rich muscovite		
11-3B	Wall	+9.8	2399	10
16-8	2nd intermediate	+11.0	4305	10.5
16-2B	3rd intermediate	+11.4	7072	9.8
16-10C	3rd intermediate	+11.1	20119	9.9
16-10C replicate		+10.4	15808	
18-2D	Core	+11.0	4194	9.9
18-2D replicate		+10.6	4138	
19-1B	Core	+9.8	2625	10
19-1B replicate		+8.5		
		Spodumene		
18-1C	Core	+8.3	37300	10.4
16-6	Core	+7.9	37300	10.5
15-1C	Fracture filling	+8.0	37300	11.8
15-3B	Fracture filling	+8.1	37300	10.4
		Wall zone whole rock		
WZ	10-3	+11.1	453.2	11.4
WZ	9-2	+7.5	504.3	12.1
WZ	43-1	+11.1	735.4	11.7

1. All mineral separates are the same as those used in Walker et al.(1986b) except samples 16-2B, 11-3A and 11-3C, which were drilled from rock sample during this study. The amount of drilled sample is <1 mg and dissolved in $HF+HNO_3$ without any cleaning.
2. Analytical uncertainty is $\leq \pm 1‰$ (2σ), based on both pure Li solutions and natural rocks (see text for details).
3. Lithium concentration measured by comparison of signal intensities with 50 or 100 ppb LSVEC, except for spodumene, which is calculated from its standard molecular formula (see text for details).
4. $\delta^{18}O$ from Walker et al (1986b).
5. Replicate: repeat column chemistry from the same stock sample solution.

Table 3. Lithium isotopic composition and concentration of fluid inclusions in quartz from the Tin Mountain pegmatite

Sample ID	Zone	δ^7Li[1]	Li (ppb)[2] leachates	Li (ppm)[3] fluid inclusions
40-6	1st intermediate	+12.5	244	2818
40-9	1st intermediate	+13.4	136	283
40-10	1st intermediate	+10.0	151	2109
40-1	1st-2nd intermediate	+9.9	163	1808
40-8	2nd intermediate	+8.1	154	3958
40-13	2nd intermediate	+11.0	143	1935
40-2	3rd intermediate-core	+10.8	104	781
40-3	Core	+10.7	204	1502

1. Analytical uncertainty is $\leq \pm$ 1‰ (2σ), based on both pure Li solutions and natural rocks (see text for details).
2. The Li concentrations in the leachates (bulk fluid extracted from 4 g of quartz diluted in 4 ml of water) were measured by ion chromatography, with an uncertainty of < 5%.
3. Lithium concentrations in fluid inclusions were calculated based on Li and Cl concentrations in leachates measured by ion chromatography and 4.5 $NaCl_{eq}$ wt% average salinity of Tin Mountain inclusions measured by microthermometry (Sirbescu and Nabelek, 2003a).

Table 4. Lithium isotopic composition and concentration of quartz mica schists and Archean granites

Sample ID	δ^7Li[1]	Li (ppm)[2]	$\delta^{18}O$[3]
Proterozoic schists			
23-2	+2.5	68	11.8
40-1A	-3.1	62	12.5
WC-4	+1.6	79	13.7
26-2	+2.3	150	12.3
Archean granites			
39-1 (Bear Mountain)	+0.1	7.7	11
41-1 (Little Elk)	-2.6	4.9	7.3

1. Analytical uncertainty is $\leq \pm$ 1‰ (2σ), based on both pure Li solutions and natural rocks (see text for details).
2. Lithium concentration measured by comparison of signal intensities with 50 or 100 ppb LSVEC.
3. Data from Walker et al (1986a).

Figure captions

Fig. 1. Map of the Black Hills, South Dakota. Locations of Proterozoic Harney Peak Granite, Tin Mountain pegmatite, Little Elk (LE) granite, Bear Mountain (BM) granite and four simple pegmatites and four Proterozoic metasediments are shown (modified from Walker et al., 1986a).

Fig. 2. Map of a vertical cross section of the zoned Tin Mountain pegmatite; the first intermediate zone doesn't crop out in this cross section; modified from Walker et al. (1989).

Fig. 3. Plots of δ^7Li versus Li for all rock and mineral samples. Data are from Tables 1,2 and 4.

Fig. 4. Plots of δ^7Li verses δ^{18}O, SiO_2, Li, and Rb for Harney Peak Granite. Data are from Table 1, Walker et al (1986a; 1989) and Nabelek et al (1992a).

Fig. 5. δ^7Li and Li concentration for minerals and fluid inclusions in different zones of the Tin Mountain pegmatite. Pl = plagioclase, Ms = muscovite, Spd = spodumene, Qtz = Quartz. Data are from Tables 2 and 3.

Fig. 6. Lithium isotopic fractionation modeled by Rayleigh distillation during: a) crystal-melt fractionation and b) fluid exsolution. Equations and variables used: $\delta^7Li_m = (\delta^7Li_i + 1000)f^{(\alpha-1)} - 1000$; $C_m = C_i(1-F)^{D-1}$; $\alpha = {}^7Li/{}^6Li_{fluid\ (crystal)} / {}^7Li/{}^6Li_{melt}$; $D = Li_{fluid\ (crystal)}$ /

Li_{melt}; f: the fraction of Li remaining in the melts; F: fraction of crystal or fluid removed. m: remaining melt; *i*: initial melt. Numbers on lines represent different D values. Shaded areas represent measurement uncertainty (± 1‰, 2σ).

Fig. 7. Plot of δ^7Li versus Rb for the wall zone whole rocks of the Tin Mountain pegmatite, simple pegmatites, Harney Peak Granite and schists. Data are from Tables 1, 2, 4 and Walker et al (1986b; 1989).

Fig. 8. Plot of δ^7Li versus Li for quartz and fluid inclusions from the Tin Mountain pegmatite. Data are from Tables 2 and 3. Star represents inclusion-free quartz (δ^7Li = 27 ± 2.1, 2σ) from Lynton et al (2005).

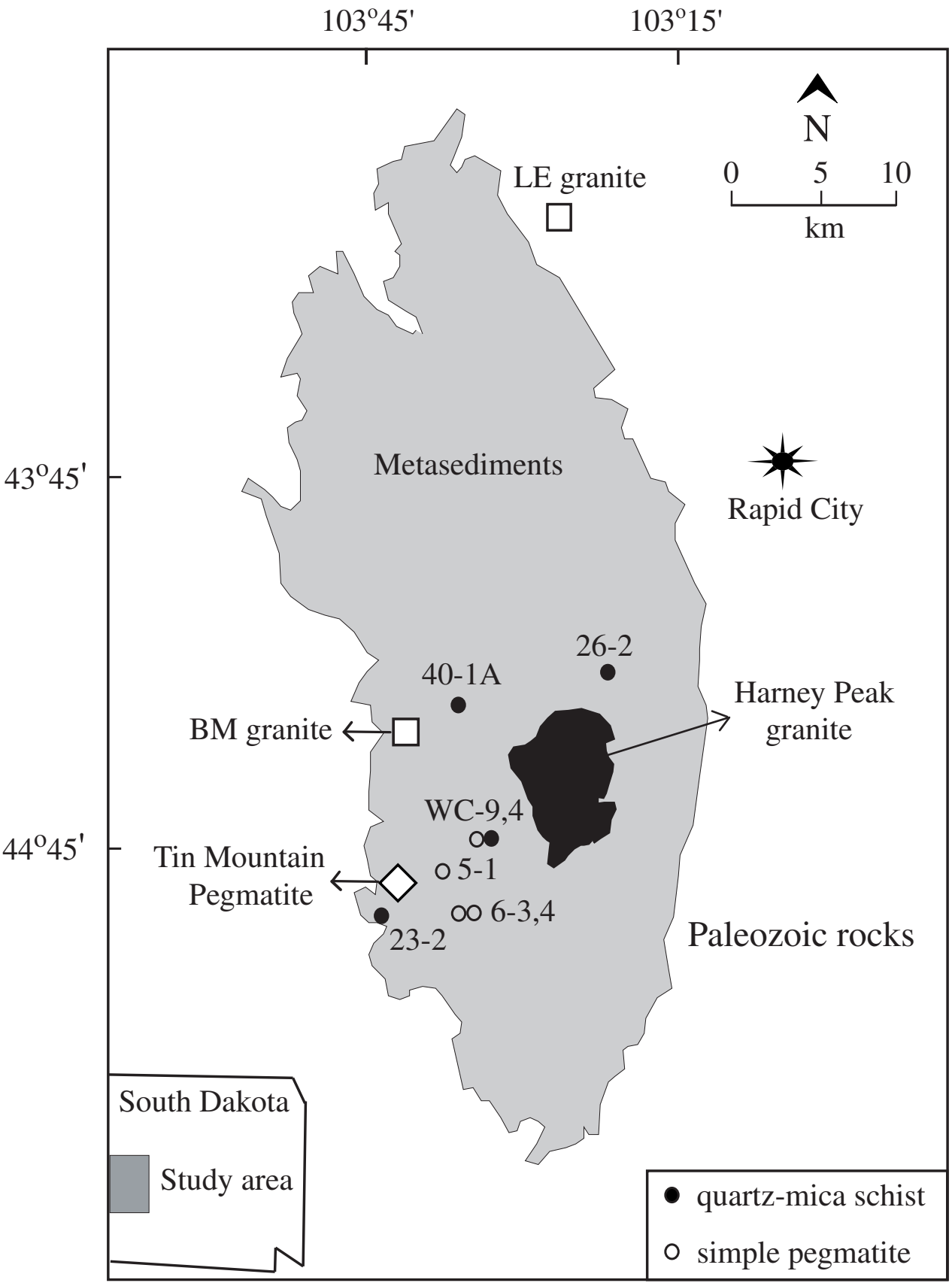

Figure 1. Teng et al. 2005

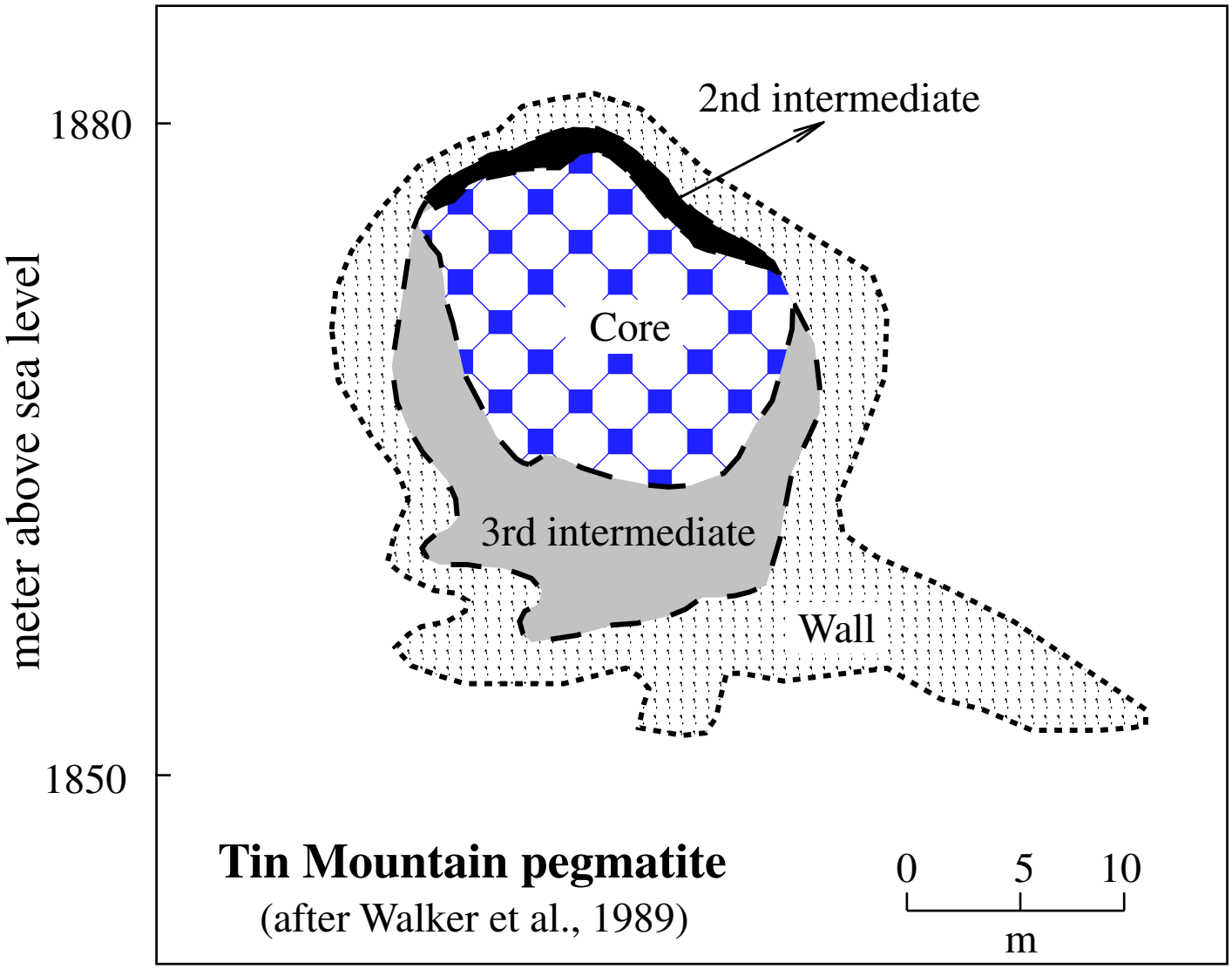

Figure 2

Teng et al. 2005

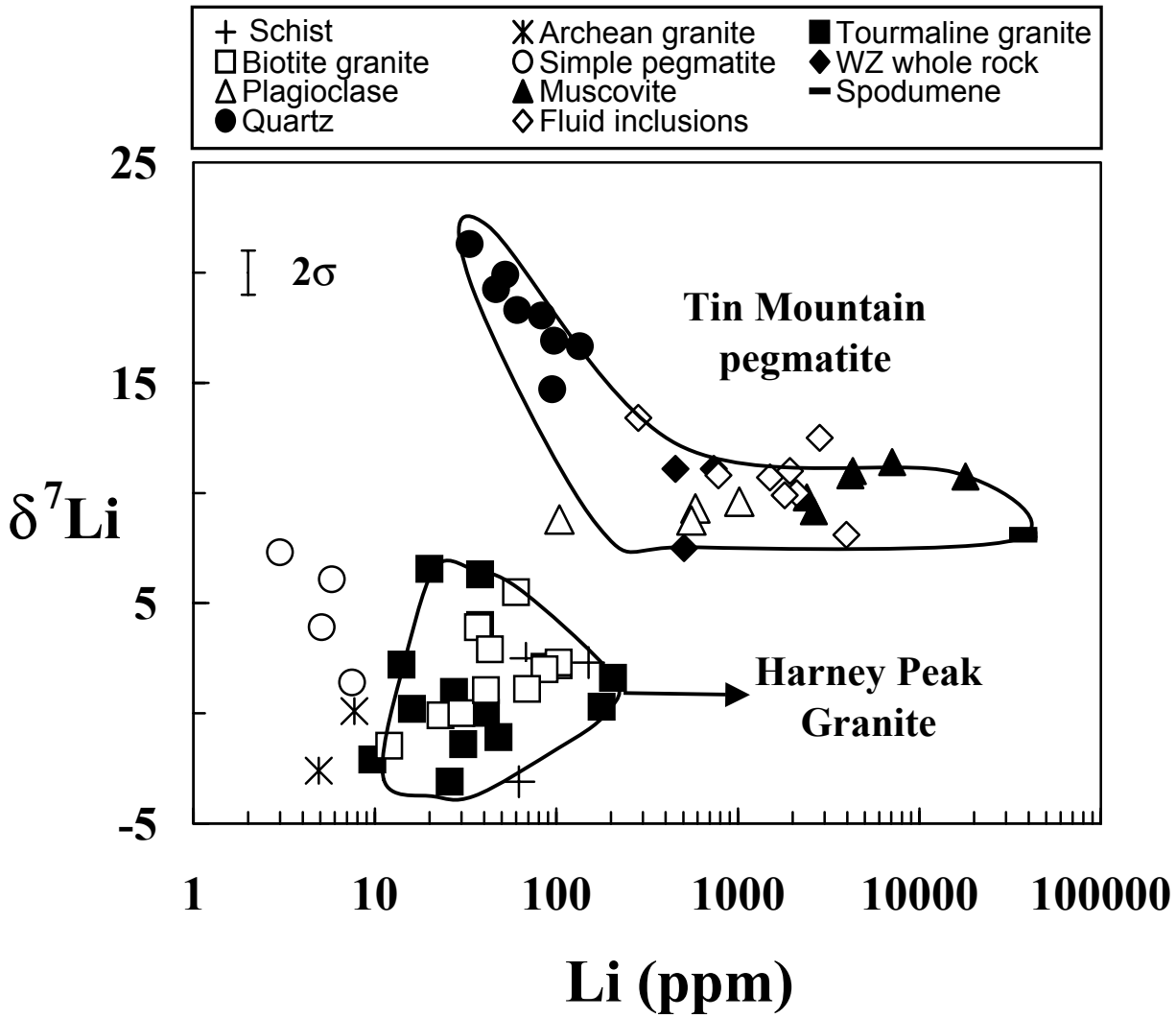

Figure 3 Teng et al 2005

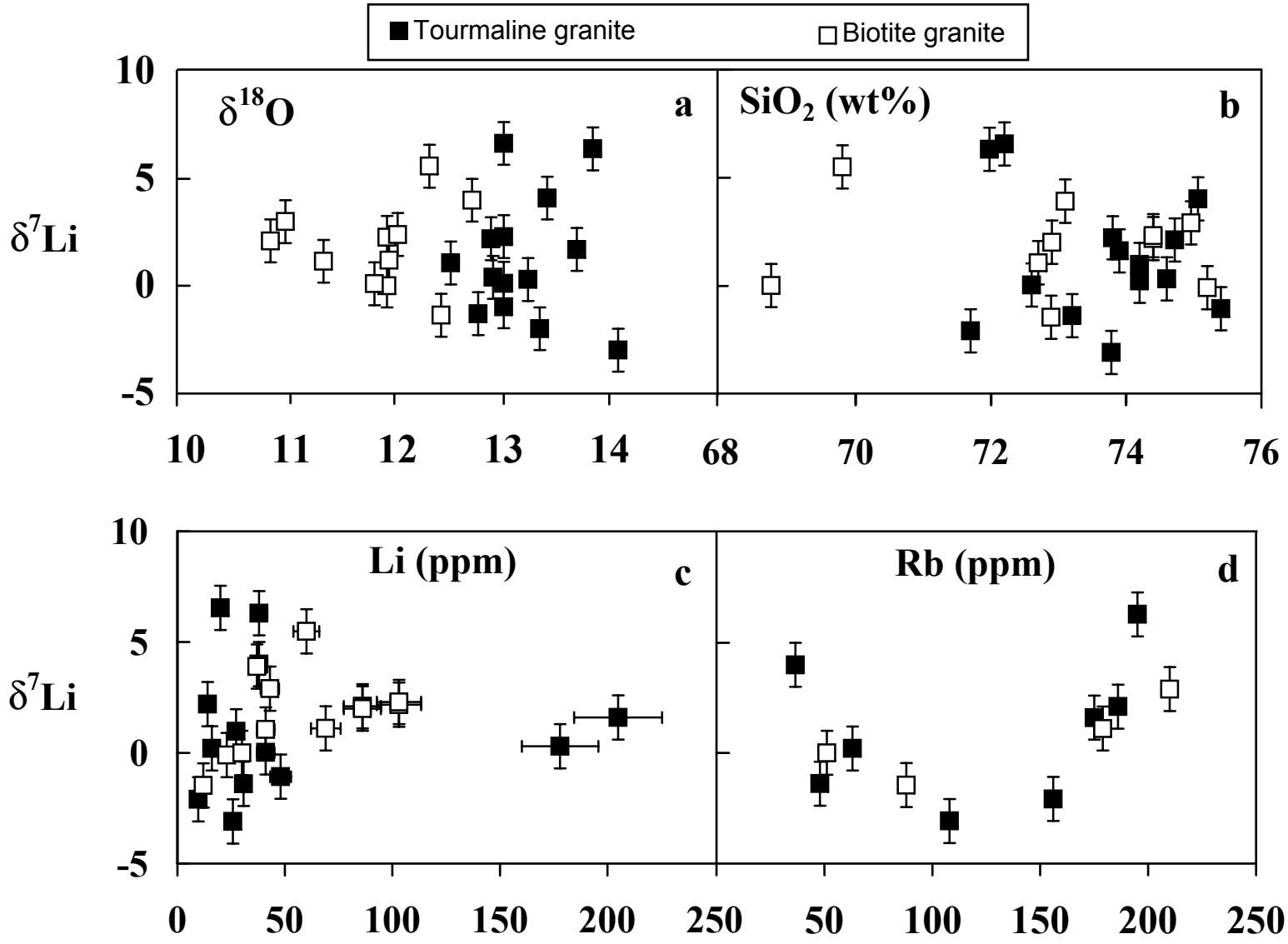

Figure 4

Teng et al 2005

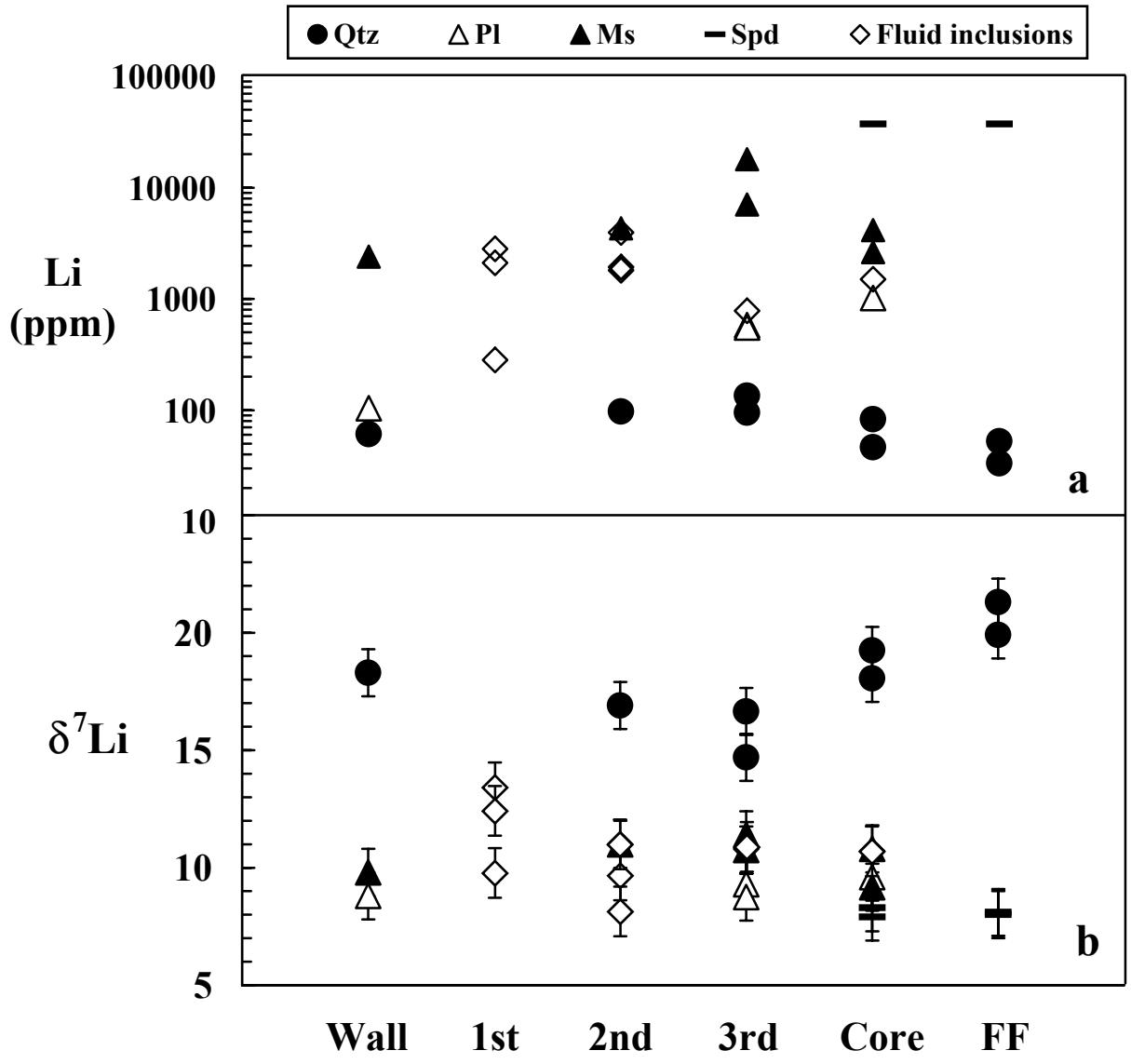

Figure 5 Teng et al.

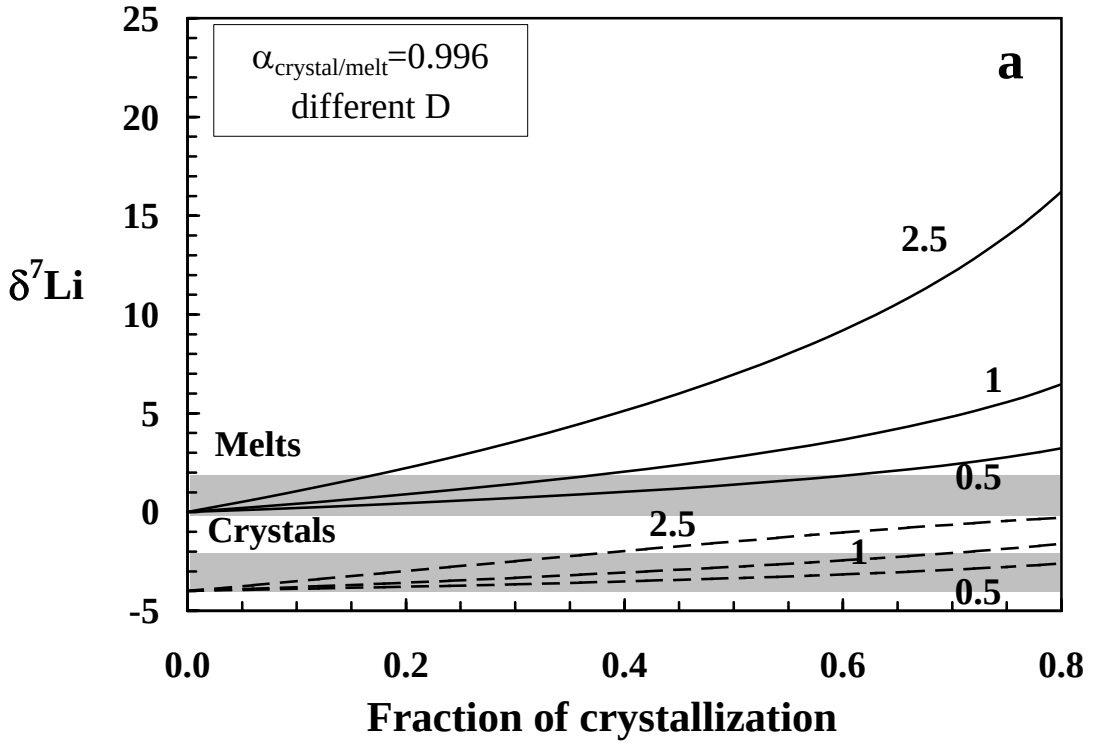

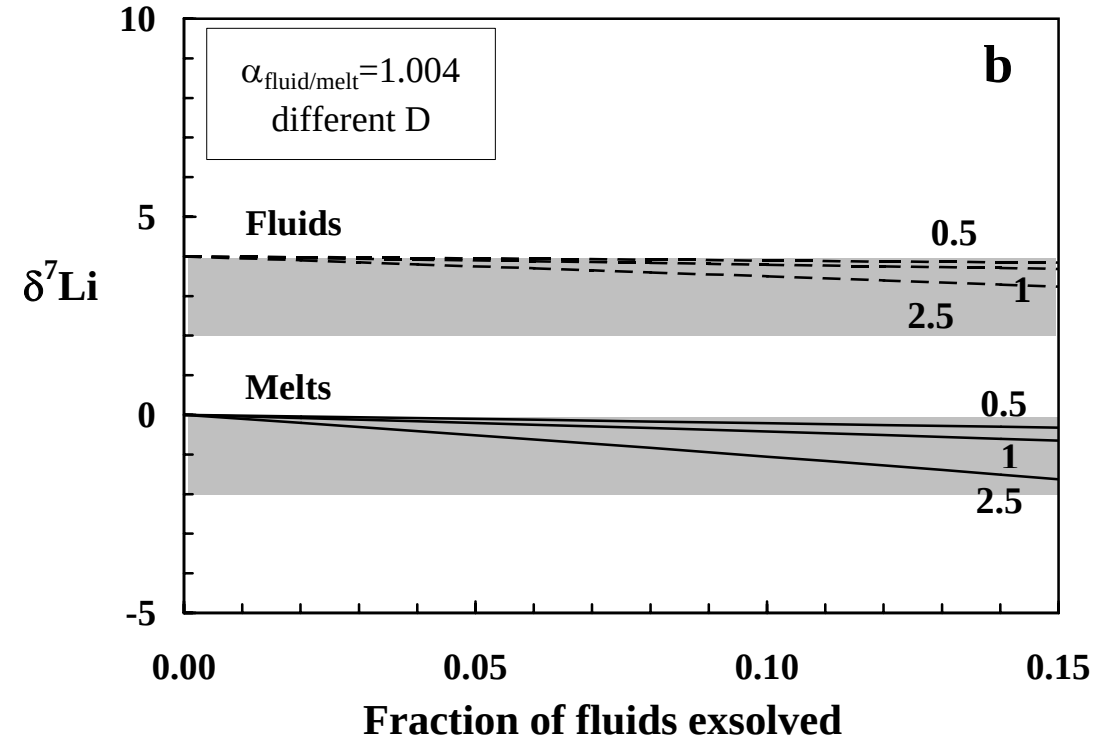

Figure 6 Teng et al. 2005

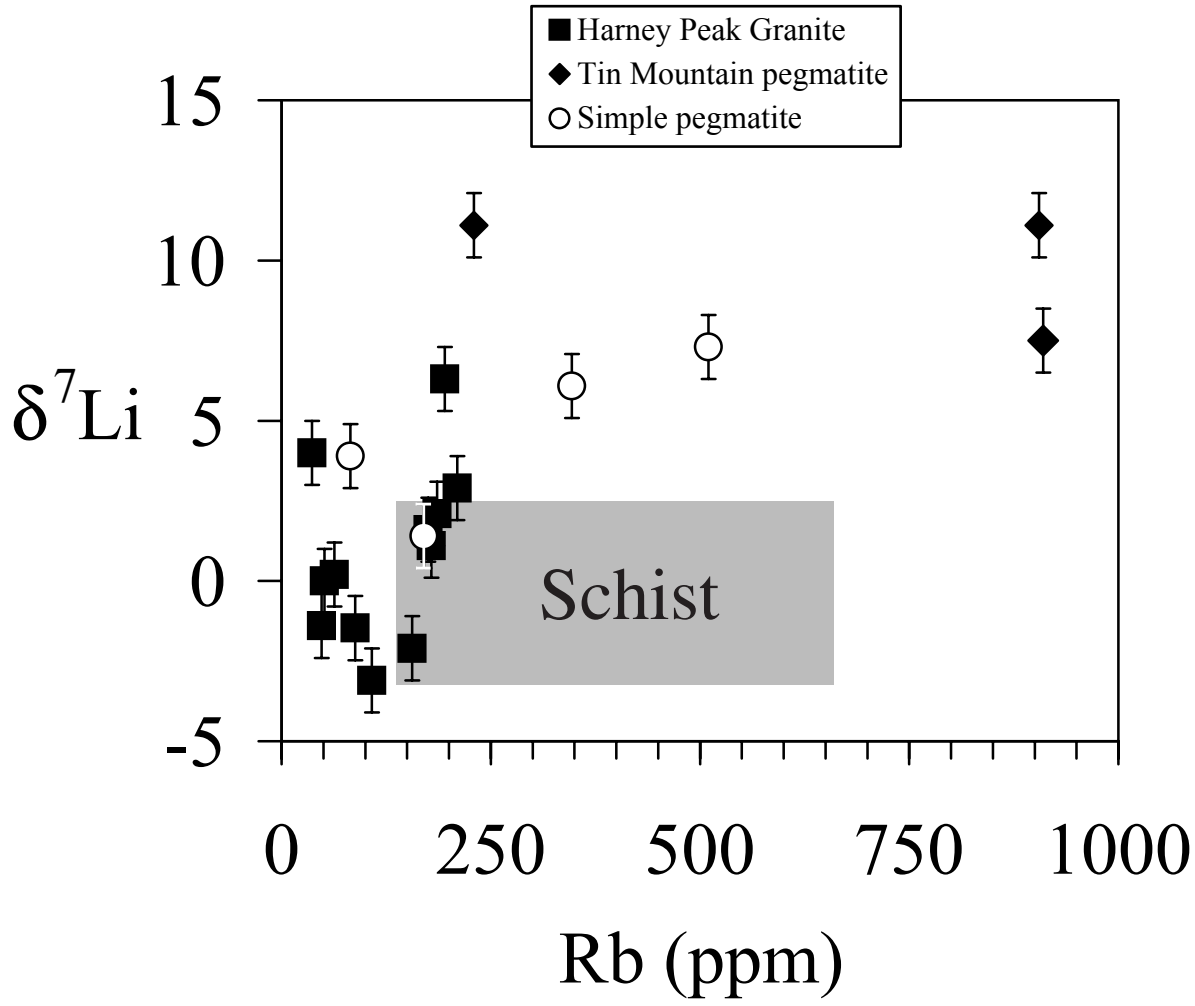

Figure 7 Teng et al 2005

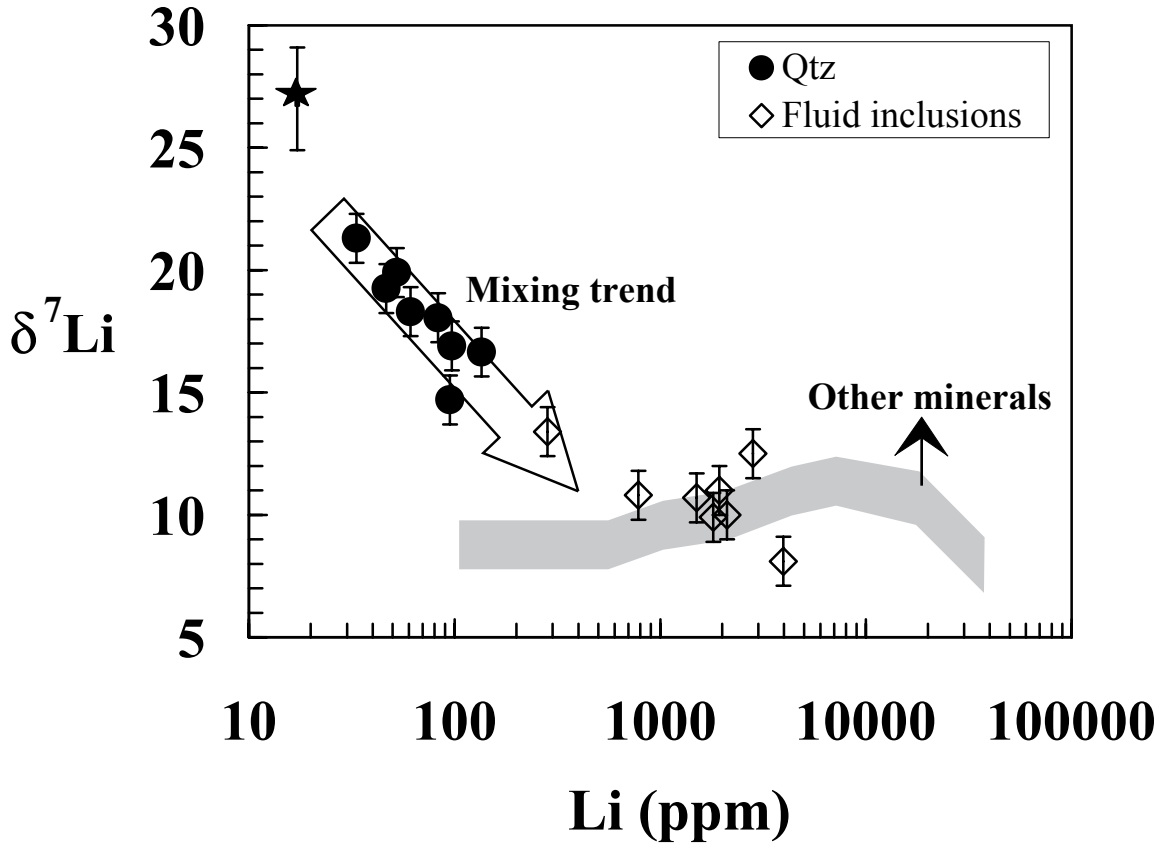

Figure 8 Teng et al 2005